CO Adsorption-Driven Surface Segregation of Pd on Au/Pd Bimetallic Surfaces: Role of Defects and Effect on CO Oxidation

Hyun You Kim[†],* and Graeme Henkelman*

Department of Chemistry, University of Texas at Austin, Austin, Texas 78712-0165, United States

Ⓢ *Supporting Information*

ABSTRACT: We use density functional theory (DFT) to study CO-adsorption-induced Pd surface segregation in Au/Pd bimetallic surfaces, dynamics of Pd–Au swapping, effect of defects on the swapping rate, CO-induced Pd clustering, and the reaction mechanism of CO oxidation. The strong CO-philic nature of Pd atoms supplies a driving force for the preferential surface segregation of Pd atoms and Pd cluster formation. Surface vacancies are found to dramatically accelerate the rate of Pd–Au swapping. We find that Pd clusters consisting of at least four Pd atoms prefer to bind O_2 rather than CO. These clusters facilitate the rapid dissociation of O_2 and supply reactive oxygen species for CO oxidation. Our findings suggest that geometric, electronic, and dynamic effects should be considered in the function of bimetallic alloys or nanoparticles whose components asymmetrically interact with reacting molecules.

KEYWORDS: *density functional theory, gold, palladium, heterogeneous catalysis, adsorption-induced segregation, CO oxidation*
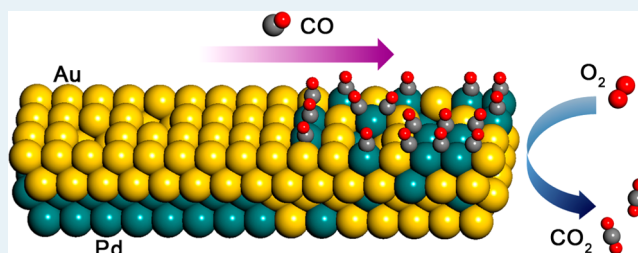
1. INTRODUCTION

The catalytic activity of bimetallic alloys or nanoparticles (NPs) can be optimized by controlling structural factors, such as the alloying element and concentration.[1,2] The ensemble (geometric) and ligand (electronic) effects have been shown to systematically alter the catalytic activity of bimetallic catalysts.[3,4]

Computational methods such as density functional theory (DFT) can effectively aid the design of bimetallic catalysts at the atomic scale.[5–10] Computational approaches generally assume that the thermodynamically most favorable structure of clean bimetallic catalysts is stable. Experiments, however, question the generality of this assumption. Somorjai and co-workers reported that the core and shell elements of Pd (core) @Rh (shell) NP are reversible under ambient reaction conditions.[11,12] Using ambient-pressure X-ray photoelectron spectroscopy, they showed that as the Pd@Rh NPs supported on oxidized silicon wafer oxidize CO with NO ($2CO + 2NO \rightarrow 2CO_2 + N_2$), Pd is enriched in the surface layers, leading to a structural rearrangement to the Rh@Pd reverse core–shell geometry. The original Pd@Rh core–shell structure was recovered when CO was removed from the gas phase. Chen and co-workers reported such a CO-induced Pt segregation in TiO_2-supported Pt–Au NPs, as well.[13]

In the case of bimetallic surfaces, the Goodman group reported that Pd segregated to the surface layer as Au overlayered-Pd(100) bimetallic alloys were exposed to CO oxidation conditions.[14,15] More Pd was segregated in the surface layer as the CO partial pressure was increased. The surface segregated Pd atoms were found to catalyze CO oxidation, and the authors suggested that contiguous Pd atoms in the surface layer provided the catalytically active site. Their rationale was that contiguous Pd atoms bind and dissociate the O_2 molecule supplying O atoms for CO oxidation.

Since adsorption- or reaction-induced surface segregation of a specific element in bimetallic alloys and NPs affects their chemical properties, information on the reaction- or adsorption-induced surface segregation is important for catalyst design.

Interatomic swapping of core and shell elements reported in Pd- or Pt-based bimetallic catalysts is presumably driven by an asymmetrically strong CO adsorption on Pd or Pt atoms.[13–16] DFT results presented by Soto-Verdugo and Metiu showed that CO prefers to bind on Pd rather than on Au in Au/Pd bimetallic alloys.[16] The same trend was reported for Pt/Au NPs by Chen and co-workers.[13] Although several previous reports on the CO-induced preferential surface segregation suggested that the strong CO binding on Pd or Pt induces the atomic swapping, detailed information on the swapping process is still sketchy.

Here, we demonstrate the dynamics of the CO-adsorption-driven Pd–Au swapping, Pd surface segregation, that occurs in the Pd–Au(111) and Pd–Au(100) bimetallic alloys. We found that the relatively strong CO binding on Pd, as compared with that on Au, stabilizes the Pd–CO* in the surface layer and supplies a driving force for Pd surface segregation. Surface Au vacancies accelerate the Pd–Au swapping, highlighting the essential role of defects on the swapping dynamics. The
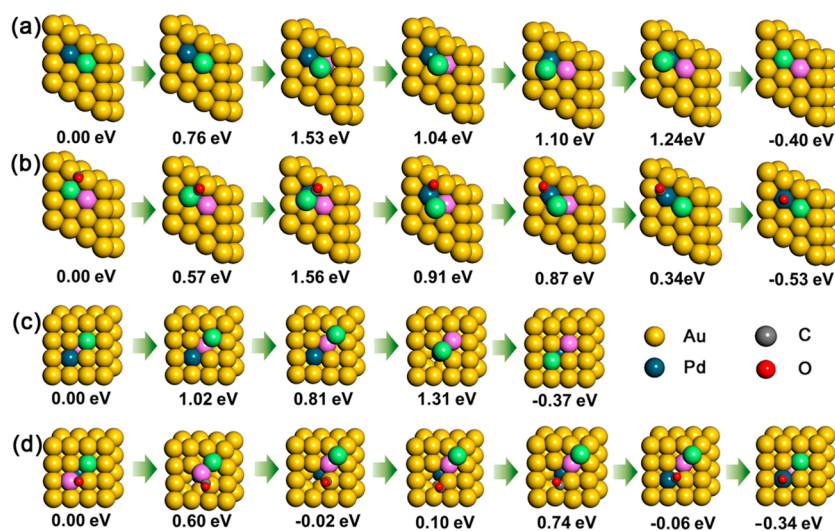
Figure 1. Pd−Au swapping process and relative energy of swapping intermediates in clean Pd−Au surfaces: (a) Pd−Au(111), (b) Pd−Au(111)−CO, (c) Pd−Au(100), and (d) Pd−Au(100)−CO. The relative energy of the intermediates was calculated relative to the unstable position of the Pd atom. The Pd−Au swapping proceeds from left to right, stabilizing the system. Au atoms involved in the swapping process are colored in light green and pink.

morphology of reactive species and the role of the Pd concentration on the CO oxidation mechanism are discussed.

2. COMPUTATIONAL METHOD

We performed spin-polarized DFT calculations in a plane-wave basis with the VASP code[17] and the PBE GGA functional.[18] Valence electrons were described by plane waves up to an energy cutoff of 290 eV, and the core electrons were described within the projector augmented wave framework.[19] To study the Pd−Au swapping mechanism, 4 × 4 Au(111) and Au(100) slabs with four atomic layers and 20 Å of vacuum thickness were constructed. A single subsurface Au atom was substituted with a Pd atom to give an in-plane Pd concentration of 1/16 = 6.25%. The top two surface layers were relaxed during geometric optimization. We used a 2 × 2 × 1 k-points grid sampling of the Brillouin zone for all calculations. Sensitivity tests show that our results are robust with respect to the calculation and model parameters, including the choice of oxygen pseudopotential, k-point grid, cutoff energy, and size and thickness of the slab (see Supporting Information Table S1 for details). The energy of CO adsorption on the Pd−Au(100) calculated with a harder oxygen pseudopotential and an energy cutoff of 500 eV was changed by only 0.07 eV.

Final convergence criteria for the electronic wave function and geometry were 10^{-4} eV and 0.01 eV/Å, respectively. We used the Gaussian smearing method with a width of 0.2 eV to improve convergence with respect to states near the Fermi level. The location and energy of transition states (TSs) were calculated with the climbing-image nudged elastic band method[20,21]

3. RESULTS AND DISCUSSION

3-1. Energetics of Pd−Au Swapping in Clean Surfaces.
In vacuum, a Au-covered Pd overlayer is the thermodynamically most stable configuration of the Au/Pd bimetallic alloy.[22] Figure 1a, c and Table 1 present the process of Pd−Au swapping in both clean Pd−Au(111) and Pd−Au(100) surfaces, the driving force and the activation energy barrier (E_b), and the approximate rate of swapping is calculated at 300

Table 1. Pd−Au Swapping Energy Barrier (E_b) and the Approximate Rate of Pd−Au Swapping Calculated at 300 K with Harmonic-Transition State Theory, Assuming a Standard Prefactor of $\nu = 10^{12}$ s^{-1a}

	Pd−Au(111)	Pd−Au(111)−CO	Pd−Au(111)-Vac	Pd−Au(111)-Vac−CO
E_b (eV)	1.53	1.56	0.73	0.81
rate (s^{-1})	1.98×10^{-14}	6.21×10^{-15}	5.45×10^{-1}	2.47×10^{-2}

	Pd−Au(100)	Pd−Au(100)−CO	Pd−Au(100)-Vac	Pd−Au(100)-Vac−CO
E_b (eV)	1.31	0.76	0.42	0.51
rate (s^{-1})	9.84×10^{-11}	1.71×10^{-1}	8.80×10^{4}	2.71×10^{3}

$^a E_b$ and the rate of Pd−Au swapping were calculated to the direction that lowers the energy of the system.

K with harmonic-transition state theory, assuming a standard prefactor of $\nu = 10^{12}$ s^{-1}. A Pd atom thermodynamically prefers the subsurface layer, as compared with the surface layer. The Pd−Au swapping process, the barrier, and the rate have been calculated in the direction where the Pd−Au swapping stabilizes the system, swapping a surface Pd atom with a subsurface Au atom.

In both cases, an adjacent surface Au atom to the Pd atom moves onto the surface to become an adatom, to make space (a vacancy) for the Pd−Au swapping process. Adatom/vacancy formation is a high-energy process, and the energy barrier for Pd−Au swapping is also (comparably) high. The swapping barrier of the more open Pd−Au(100) surface is only somewhat lower than that of the close packed Pd−Au(111) (1.31 and 1.53 eV, respectively, as listed in Table 1). The low calculated rates confirm that, in the case of clean surfaces, Pd atoms would be pinned to their original positions at low temperature; even the Pd subsurface segregation is thermodynamically favorable (Table 1). Measurable swapping rates of 10 s^{-1} are achievable at 650 K for Pd−Au(111) and 470 K in Pd−Au(100), respectively.

We found that two Pd atoms in the surface layer repel and favor being separated from each other. The formation energy of a Pd−Pd dimer from two separated Pd atoms is 0.1 eV, meaning that Pd cluster formation is unfavorable. Configurational entropy would additionally destabilize the Pd−Pd dimer at low Pd surface concentrations. The swapping barrier of the second Pd atom in the presence of a preswapped Pd atom in the surface layer would be higher than the barrier of the first swapping.

On the other hand, strong CO binding to Pd stabilizes the Pd−CO* complex in the surface layer and supplies a driving force for the Pd surface segregation. (Figure 1b, d and Table 1). CO lowers the E_b of Pd surface segregation, especially in the case of Pd−Au(100). Presumably, relatively stronger CO binding on the Au(100) surface (−0.63 eV, Au−Au bridge position) than the Au(111) surface (−0.25 eV, 3-fold hollow position) lowers the energy of swapping intermediates in the Pd−Au(100)−CO complex. However, the Pd−Au swapping still requires an adatom formation in both cases, so the E_b is still high (Table 1). Although CO exchanges the stable location of Pd, the Pd−Au swapping is a rare event, even in the presence of CO.

3-2. Energetics of Pd−Au Swapping in Defected Surfaces.

In their polarization−modulation infrared reflection adsorption spectroscopy (PM-IRRAS) study on the well-annealed and freshly ion-sputtered Au-overlayered Pd(100), Goodman and co-workers reported that CO-induced Pd surface segregation is more prominent in the freshly ion-sputtered Au/Pd(100) surface.[15] Contiguous Pd atoms, a result of high Pd surface concentration, were observed in the freshly sputtered specimen, even when it was exposed to very low CO partial pressure (1×10^{-6} Torr). On the other hand, higher CO partial pressure is required for the formation of contiguous Pd atoms in the well-annealed specimen.[15] This finding suggests a critical effect of surface roughness or defects for the dynamics of the Pd−Au swapping. Moreover, recent experimental findings on the structure of Au/Pd bimetallic NPs confirm the presence of surface vacancies in small NPs, as well.[23,24] HRTEM studies by Xu et al. showed that vacancies appear in the surface layer of Pd−Au NPs.[24] Meija-Rosales et al. experimentally observed surface vacancies in Au−Pd NPs and confirmed the structure by molecular dynamics simulations.[23] These findings suggest the consideration of a defect on the Pd−Au swapping processes by introducing a Au surface vacancy.

Figure 2a, c shows that a Au vacancy facilitates the Pd−Au swapping pathway without adatom formation or surface distortion. A Au vacancy in the surface layer of the Pd−Au(111)-Vac and Pd−Au(100)-Vac, therefore, lowers the swapping energy barriers (Table 1). Pd penetration from the surface layer to the subsurface layer is the rate-determining step due to the relatively low energy of the intermediate structure: the Au/Pd surface with a subsurface Au vacancy.

Figure 2b, d shows that the preferential CO adsorption on Pd again stabilizes the Pd−CO* complex in the surface of the defected Pd−Au(111)-Vac−CO and Pd−Au(100)-Vac−CO, leading to surface segregation of Pd. The presence of CO again supplies a driving force for Pd surface segregation but does not accelerate the Pd−Au swapping (Table 1).

In the case of the Pd−Au(111)-Vac systems (Figure 2a, b) DFT predicts a structure with a subsurface Au vacancy and a Pd in the surface layer as a more stable structure than the final state with a surface vacancy. A similar result was acquired for the clean Au(111) surface, as well; the result is insensitive to the
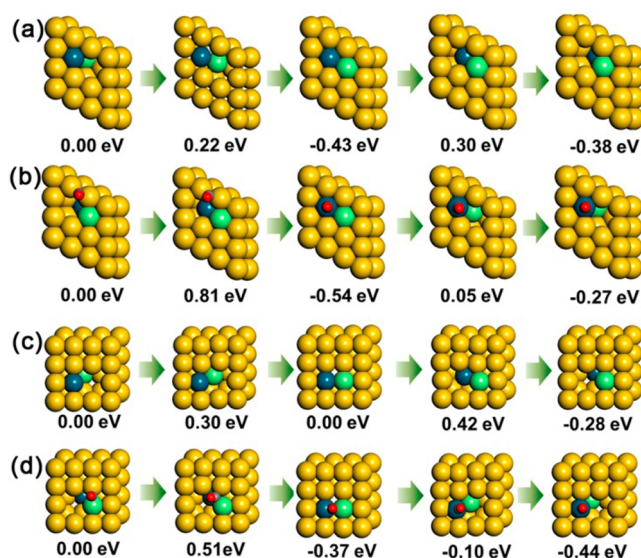

Figure 2. Pd−Au swapping process and relative energy of swapping intermediates in defected Pd−Au surfaces: (a) Pd−Au(111)-Vac, (b) Pd−Au(111)-Vac−CO, (c) Pd−Au(100)-Vac, and (d) Pd−Au(100)-Vac−CO. Relative energy of intermediates was calculated relative to the unstable position of the Pd atom. The Pd−Au swapping proceeds from left to right, stabilizing the system. A Au atom involved in the swapping process is colored in light green.

calculation parameters, including k-points grid, energy cutoff, and slab thickness. This is a somewhat surprising result because the subsurface vacancy generates more dangling bonds than the surface oxygen vacancy. However, because the formation of the surface Pd−CO* is insensitive to the location of the Au vacancy, the main conclusions reached here are not affected.

Our findings confirm that, under CO oxidation conditions, CO supplies a driving force for the preferential surface segregation of CO-philic Pd atoms in the Au/Pd bimetallic alloys so that the local geometry of the Au/Pd bimetallic alloys could be different from their thermodynamically most stable structure. Although CO molecules affect the Pd−Au swapping barrier, we find that the vacancy critically accelerates the Pd−Au swapping (Table 1).

3-3. Multiadsorption of CO on Pd Atoms and Subsequent Pd Clustering.

Goodman and co-workers reported that the Au/Pd(100) surface alloy catalyzes CO oxidation as contiguous Pd atoms in the surface layer dissociates O_2 molecules.[14,15] As experimental evidence, they resolved PM-IRRAS data acquired at 100 K and reported IR peaks of the bridging CO species, Pd−CO*−Pd, at 1999, 1976, and 1908 cm^{-1}. These peaks are located below 2000 cm^{-1}, whereas the peak that corresponds to Pd−CO* lies at 2085 cm^{-1} (Figure 3a).

DFT-calculated IR frequencies of the Pd−CO*−Pd were found at 1910, 1904, and 1902 cm^{-1}, which are in good agreement with the experimental value of 1908 cm^{-1} (Figure 3d, e). We found that the experimental peak at 1999 cm^{-1} is coming from the harmonics between adjacent two Pd−CO* species (see Figure 3c). The experimentally reported IR peak at 1976 cm^{-1} is likely due to bridge CO molecules bound to Pd atom clusters. We found a frequency at 1930 cm^{-1} (Figure 3e) in a Pd_6 cluster model. Additional subsurface Pd atoms would shift these values to higher energies. DFT-calculated IR frequencies of weakly bound Pd−CO*−Au species were found at 1893 and 1891 cm^{-1} (Figure 3b, d, and e). These
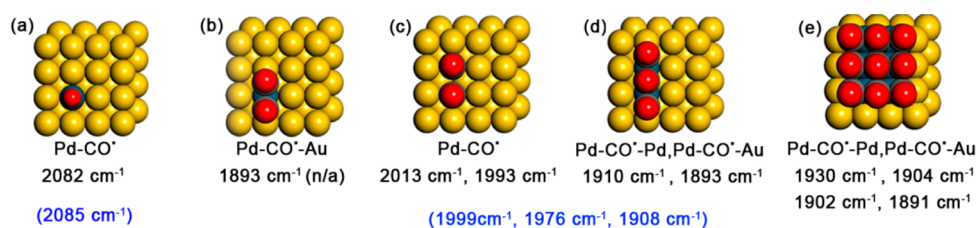
Figure 3. DFT calculated IR frequencies of surface CO species: (a, b) Pd monomer, (c, d) Pd dimer, and (e) Pd cluster consisting of six Pd atoms. Values in parentheses show experimental IR data.[14,15]

modes, however, would disappear as the Pd—CO* and Pd—CO*—Pd become a dominant species, at increased Pd concentrations.

Given the well-known CO binding nature on CO-philic metal surfaces (single CO adsorption on a metal atom), CO stripping has been used to determine the surface coverage of CO-philic metal elements of bimetallic systems.[25] Galhenage et al. found that the surface concentration of Co, Ni, or Pt of Au-based bimetallic clusters supported on TiO$_2$ estimated by CO temperature-programmed desorption is greater than that from a low-energy ion scattering experiment.[25] We postulate that the presence of the bridge-bound CO is attributed to the overestimated surface concentration of the CO-philic element estimated by CO temperature-programmed desorption.

Soto-Verdugo and Metiu showed that the repulsive force between adjacent Pd—CO*'s is low; Supporting Information Figure S1 confirms their finding.[16] Because the binding energy of the bridging CO molecule (Pd—CO*—Pd) is higher than the on-top Pd—CO* molecule, as Pd atoms segregate to the surface (see Figure 4), these bridge-bound CO molecules would promote Pd clustering.
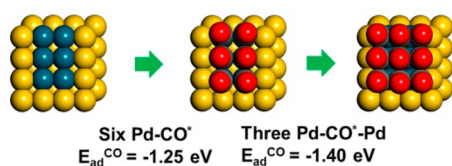

Figure 4. Strong binding of Pd—CO*—Pd on the Pd$_6$ cluster. The stronger binding of the final three CO molecules supplies a driving force for Pd clustering.

3-4. CO Oxidation by Pd Motifs. To provide insight into the reactive species, we studied CO oxidation by several CO species at the surface of Pd—Au(100): (1) Pd monomer with a single on-top CO, Pd—CO* (M1), (2) Pd monomer with two bridging CO's, Pd—CO*—Au (M2), (3) Pd dimer with two on-top CO's, Pd—CO* (D1), and (4) Pd dimer with three bridging CO's, one bridging Pd—CO*—Pd, and two bridging Pd—CO*—Au's (D2). Refer to Figure 5 for the detailed geometry of these models. We found, however, that these species cannot bind O$_2$ strongly enough to catalyze CO oxidation. Under CO oxidation conditions, M1 would prefer to bind an additional CO molecule ($E_b = -0.96$ eV), forming the M2 structure rather than binding an O$_2$ molecule with a lower (-0.44 eV) binding energy. In the case of M2, the available Pd sites are already saturated by CO molecules so that coadsorption of O$_2$ with the two CO molecules (-0.27 eV) is weak. Note that the binding energy of O$_2$ on M2 is lower than the entropic contributions to the free energy of O$_2$ desorption, -0.64 eV (the entropic contribution to the Gibbs free energy of O$_2$ desorption at the conventional operating temperature of CO oxidation is -0.64 eV at 298 K and 1 bar; the standard entropy of O$_2$ at 298 K is 205.14 J mol^{-1} K^{-1}),[26,27] confirming that additional binding of O$_2$ on M2 is not favorable (see the Supporting Information for details). D1 would prefer to bind additional CO ($E_b = -1.21$ eV) rather than O$_2$ ($E_b = -0.69$ eV). Weak O$_2$ binding at D2 ($E_b = -0.22$ eV) also shows that D2 is not a good catalyst geometry for CO oxidation. CO oxidation by a catalyst that weakly binds O$_2$ and cannot supply a reactive O* species usually follows the Langmuir—Hinshelwood mechanism, requiring the association of coadsorbed CO* and O$_2$*.[9,10,28−30] Results show that isolated Pd atoms or dimers cannot activate CO oxidation by the association of coadsorbed CO* and O$_2$*.

Table 2 shows that the binding preference of the Pd cluster changes from CO to O$_2$ as the Pd cluster is composed of more than four Pd atoms; Pd$_4$ and Pd$_6$ clusters strongly bind O$_2$. Because DFT calculations at the GGA level of theory have systematic errors in the binding energy of O$_2$ and CO, the relative binding energies (for example, ΔE_{ad} in Table 2) are expected to be more accurate than the absolute values. The qualitative trend in the value of ΔE_{ad}, changing from positive to negative at Pd$_4$, leads us to conclude that the binding of O$_2$ is favored over CO in Pd clusters larger than Pd$_4$. Moreover,
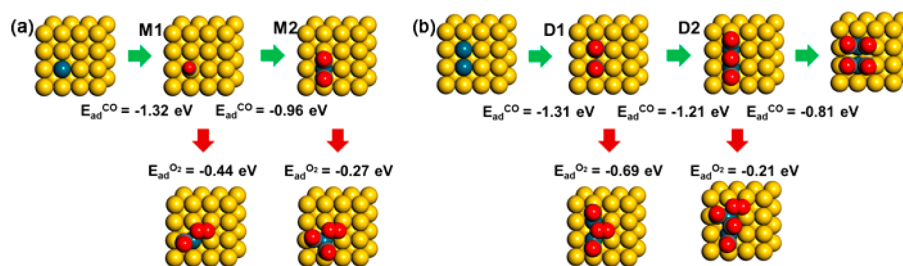
Figure 5. Trends in competitive CO and O$_2$ binding on the Pd monomer (a) and Pd dimer (b) in the Pd—Au(100) surface. Pd monomer and dimer prefer to bind CO molecules as much as possible (green arrows) rather than binding an O$_2$ molecule with CO molecules (red arrows). The associative mechanism of CO oxidation,[9,10,28] CO oxidation by coadsorbed O$_2$ and CO is not the case of the Pd monomer and dimer.

Table 2. Trends in CO Adsorption and O_2 Adsorption and Dissociation on Pd_x Clusters^a

	Pd_1	Pd_2	Pd_4	Pd_6
E_{ad}^{CO} (eV)	−1.14	−1.17	−1.28	−1.30
$E_{ad}^{O_2}$ (eV)	−0.77	−1.06	−1.57	−1.66
$\Delta E_{ad} = E_{ad}^{O_2} - E_{ad}^{CO}$	0.37	0.09	−0.29	−0.36
O_2 dissociation energy (eV)	n/a	n/a	0.04	−0.86
E_b (eV)	n/a	n/a	0.28	0.16

$^a E_{ad}^{CO}$, $E_{ad}^{O_2}$, and E_b denotes average energy of CO adsorption, energy of O_2 adsorption, and O_2 dissociation barrier, respectively. Pd_x is a Pd cluster composed of x Pd atoms on the Pd−Au(100) surface. E_{ad}^{CO} was calculated with two, four, six, and nine bound CO molecules to Pd_1, Pd_2, Pd_4, and Pd_6, respectively.

clustering of Pd atoms lowers the activation energy of O_2 dissociation, leading to easier O_2 dissociation and promoting subsequent CO oxidation by highly reactive O* that oxidizes CO by the Langmuir−Hinshelwood mechanism or the Eley−Rideal mechanism (refer to Supporting Information Figure S2 for detailed geometries of O_2 adsorption and dissociation of Pd_4 and Pd_6).[9,10] We postulate that although some CO molecules on the Pd atoms of Pd clusters that drive Pd surface segregation would be removed from the surface as a result of CO oxidation, Pd clusters would stay in the surface layer under CO oxidation condition as a result of strong O_2 binding to the Pd clusters. Because the CO oxidation in this system is catalyzed by Pd motifs larger than Pd_4, the overall CO oxidation reactivity would converge to those of the pure Pd (100) surface.

Given the stronger CO binding energy of Pd motifs smaller than Pd_4 (see Table 2), CO binding on a Pd atom initially supplies a driving force for Pd surface segregation. As the size of Pd motifs increase larger than Pd_4, the strong oxygen binding on Pd motifs larger than Pd_4 would attribute to further Pd surface segregation, as well.

Because the Au−Pd catalyst is exposed to CO oxidation conditions (a mixture of CO and O_2), the reduction of the Pd−O* by CO would be very fast (by the Eley−Rideal mechanism). The PdO oxide islands, therefore, would not be stabilized (the life span of the oxide at the surface layer of Pd−Au alloy would be short). Even though ideal theoretical calculations could predict the formation of PdO islands in oxygen-rich conditions, it would not be the case of the real CO oxidation conditions.

4. SUMMARY

According to conventional computational catalyst design methods, which have focused on ensemble and ligand effects, a low concentration of Pd in a Au alloy would not likely be regarded as a catalyst for CO oxidation because Au surface atoms cannot bind and dissociate O_2. Herein, we suggest, however, that under CO oxidation conditions where the CO-induced Pd surface segregation occurs, the Pd−Au(100) bimetallic alloy becomes an effective CO oxidation catalyst. The strong CO-philic nature of Pd supplies a driving force for preferential surface segregation of Pd atoms, and a Au vacancy dramatically accelerates the Pd−Au swapping. This finding predicts that an adsorption-induced surface segregation would be more prominent in nanoparticles or rough surfaces, where surface atoms are less closely packed.

Pd clusters composed of at least four Pd atoms are found to be a reactive species for CO oxidation. Facile O_2 dissociation by Pd clusters is essential for high CO oxidation activity. Our

findings suggest that not only are geometric and electronic effects important, but dynamical effects also have to be considered for bimetallic alloys or NPs whose components asymmetrically interact with reacting molecules.

■ ASSOCIATED CONTENT

Ⓢ Supporting Information

Details about the DFT calculations of the free energy of O_2 binding and CO repulsion are provided. This material is available free of charge via the Internet at http://pubs.acs.org.

■ AUTHOR INFORMATION

Corresponding Author
*E-mail: hykim8083@gmail.com, henkelman@cm.utexas.edu.

Present Address
†Center for Functional Nanomaterials, Brookhaven National Laboratory, Upton, New York, 11973

Notes
The authors declare no competing financial interest.

■ ACKNOWLEDGMENTS

■ REFERENCES

(1) Crooks, R. M.; Ye, H. C. *J. Am. Chem. Soc.* **2007**, *129*, 3627−3633.
(2) Greeley, J.; Mavrikakis, M. *Nat. Mater.* **2004**, *3*, 810−815.
(3) Hammer, B.; Norskov, J. K. *Adv. Catal.* **2000**, *45*, 71−129.
(4) Gross, A. *Top. Catal.* **2006**, *37*, 29−39.
(5) Norskov, J. K.; Bligaard, T.; Rossmeisl, J.; Christensen, C. H. *Nat. Chem.* **2009**, *1*, 37−46.
(6) Greeley, J.; Stephens, I. E. L.; Bondarenko, A. S.; Johansson, T. P.; Hansen, H. A.; Jaramillo, T. F.; Rossmeisl, J.; Chorkendorff, I.; Norskov, J. K. *Nat. Chem.* **2009**, *1*, 552−556.
(7) Honkala, K.; Hellman, A.; Remediakis, I. N.; Logadottir, A.; Carlsson, A.; Dahl, S.; Christensen, C. H.; Norskov, J. K. *Science* **2005**, *307*, 555−558.
(8) Studt, F.; Abild-Pedersen, F.; Bligaard, T.; Sorensen, R. Z.; Christensen, C. H.; Norskov, J. K. *Science* **2008**, *320*, 1320−1322.
(9) Kim, H. Y.; Han, S. S.; Ryu, J. H.; Lee, H. M. *J. Phys. Chem. C* **2010**, *114*, 3156−3160.
(10) Kim, H. Y.; Kim, D. H.; Ryu, J. H.; Lee, H. M. *J. Phys. Chem. C* **2009**, *113*, 15559−15564.
(11) Tao, F.; Grass, M. E.; Zhang, Y. W.; Butcher, D. R.; Renzas, J. R.; Liu, Z.; Chung, J. Y.; Mun, B. S.; Salmeron, M.; Somorjai, G. A. *Science* **2008**, *322*, 932−934.
(12) Tao, F.; Grass, M. E.; Zhang, Y. W.; Butcher, D. R.; Aksoy, F.; Aloni, S.; Altoe, V.; Alayoglu, S.; Renzas, J. R.; Tsung, C. K.; Zhu, Z. W.; Liu, Z.; Salmeron, M.; Somorjai, G. A. *J. Am. Chem. Soc.* **2010**, *132*, 8697−8703.
(13) Tenney, S. A.; Ratliff, J. S.; Roberts, C. C.; He, W.; Ammal, S. C.; Heyden, A.; Chen, D. A. *J. Phys. Chem. C* **2010**, *114*, 21652−21663.
(14) Gao, F.; Wang, Y. L.; Goodman, D. W. *J. Phys. Chem. C* **2009**, *113*, 14993−15000.
(15) Gao, F.; Wang, Y. L.; Goodman, D. W. *J. Am. Chem. Soc.* **2009**, *131*, 5734−5735.
(16) Soto-Verdugo, V.; Metiu, H. *Surf. Sci.* **2007**, *601*, 5332−5339.
(17) Kresse, G.; Furthmuller, J. *Comput. Mater. Sci.* **1996**, *6*, 15−50.

(18) Perdew, J. P.; Burke, K.; Ernzerhof, M. *Phys. Rev. Lett.* **1996**, *77*, 3865−3868.

(19) Blochl, P. E. *Phys. Rev. B* **1994**, *50*, 17953.

(20) Henkelman, G.; Jonsson, H. *J. Chem. Phys.* **2000**, *113*, 9978−9985.

(21) Henkelman, G.; Uberuaga, B. P.; Jonsson, H. *J. Chem. Phys.* **2000**, *113*, 9901−9904.

(22) Ruban, A. V.; Skriver, H. L.; Norskov, J. K. *Phys. Rev. B* **1999**, *59*, 15990−16000.

(23) Mejia-Rosales, S. J.; Fernandez-Navarro, C.; Perez-Tijerina, E.; Blom, D. A.; Allard, L. F.; Jose-Yacaman, M. *J. Phys. Chem. C* **2007**, *111*, 1256−1260.

(24) Xu, J.; White, T.; Li, P.; He, C. H.; Yu, J. G.; Yuan, W. K.; Han, Y. F. *J. Am. Chem. Soc.* **2010**, *132*, 10398−10406.

(25) Galhenage, R. P.; Ammal, S. C.; Yan, H.; Duke, A. S.; Tenney, S. A.; Heyden, A. *J. Phys. Chem. C* **2012**, *116*, 24616−24629.

(26) Atkins, P.; Paula, J. D. *Physical Chemistry*, 8th ed.; Oxford: New York, 2006.

(27) Metiu, H. *Physical Chemistry: Statistical Mechanics*, 1st ed.; Taylor & Francis: New York, 2006.

(28) Liu, Z.-P.; Hu, P.; Alavi, A. *J. Am. Chem. Soc.* **2002**, *124*, 14770−14779.

(29) Falsig, H.; Hvolbaek, B.; Kristensen, I. S.; Jiang, T.; Bligaard, T.; Christensen, C. H.; Norskov, J. K. *Angew. Chem., Int. Ed.* **2008**, *47*, 4835−4839.

(30) Kim, H. Y.; Lee, H. M.; Henkelman, G. *J. Am. Chem. Soc.* **2012**, *134*, 1560−1570.